

Microstructure and High-Temperature Oxidation Resistance of ZrSi₂-NbSi₂ Composite Coating on Nb-Ti-Si-Cr Based Ultrahigh-Temperature Alloy (Postprint)

Authors: Li Xuan, Guo Xiping, Qiao Yanqiang

Date: 2023-03-19T00:00:00+00:00

Abstract

A ZrSi₂-NbSi₂ composite coating was prepared on the surface of a novel Nb-Ti-Si-Cr based ultra-high temperature alloy by magnetron sputtering a Zr film followed by Si-Y co-diffusion. The microstructure and formation mechanism of the coating were analyzed, and its isothermal oxidation behavior at 1250°C was investigated. The results show that coatings prepared by Si-Y co-diffusion for 4 h at 1150, 1250, and 1350°C exhibit similar microstructures, all primarily composed of a ZrSi₂ outer layer, a (Nb, X)Si₂ (X=Ti, Cr, Zr, and Hf) intermediate layer, and a (Ti, Nb)₅Si₄ inner layer. Isothermal oxidation test results demonstrate that the prepared coating possesses excellent high-temperature oxidation resistance. During oxidation, a dense oxide film consisting of a mixture of SiO₂, TiO₂, ZrSiO₄, and Cr₂O₃ formed on the coating surface, which can protect the substrate alloy from oxidation for at least 100 h in air at 1250°C.

Full Text

Preamble

ChinaXiv Cooperative Journal

Vol. 51

June 2015

No. 6 pp. 693-700

ACTA METALLURGICA SINICA

Jun. 2015 pp.693-700 Vol.51 No.6

Microstructure and High-Temperature Oxidation Resistance of ZrSi₂-NbSi₂ Composite Coatings on Nb-Ti-Si-Cr Based Ultrahigh Temper-

ature Alloys

LI Xuan, GUO Xiping, QIAO Yanqiang

(State Key Laboratory of Solidification Processing, Northwestern Polytechnical University, Xi'an 710072)

Abstract

ZrSi₂-NbSi₂ composite coatings were prepared on a novel Nb-Ti-Si-Cr based ultrahigh temperature alloy by magnetron sputtering a Zr film followed by Si-Y co-diffusion. The microstructure and formation mechanism of the coatings were analyzed, and their isothermal oxidation behavior at 1250 °C was investigated. The results show that coatings prepared at 1150, 1250, and 1350 °C for 4 h by Si-Y co-diffusion exhibit similar microstructures, consisting mainly of a ZrSi₂ outer layer, a (Nb, X)Si₂ (X = Ti, Cr, Zr, and Hf) intermediate layer, and a (Ti, Nb)₅Si₄ inner layer. Isothermal oxidation tests demonstrate that the prepared coatings possess excellent high-temperature oxidation resistance. During oxidation, a dense oxide scale composed of SiO₂, TiO₂, ZrSiO₄, and Cr₂O₃ formed on the coating surface, which protected the substrate alloy from oxidation in air at 1250 °C for at least 100 h.

Keywords

Nb-Ti-Si-Cr based ultrahigh temperature alloy, ZrSi₂-NbSi₂ composite coating, structural formation, oxidation-resistant performance

Chinese Library Classification TG174.44**Document Code** A**Article ID** 0412-1961(2015)06-0693-08**MICROSTRUCTURE AND OXIDATION BEHAVIOR OF ZrSi₂-NbSi₂ MULTILAYER COATINGS ON AN Nb-Ti-Si-Cr BASE ULTRAHIGH TEMPERATURE ALLOY**

LI Xuan, GUO Xiping, QIAO Yanqiang

State Key Laboratory of Solidification Processing, Northwestern Polytechnical University, Xi'an 710072

Correspondent: GUO Xiping, professor, Tel: (029)88494873, E-mail: xpguo@nwpu.edu.cn

Supported by National Natural Science Foundation of China (Nos.51371145, 51431003 and U1435201), Programme of Introducing Talents of Discipline to Universities of China (No.B080401) and Fund of State Key Laboratory of Solidification Processing in NWPU (No.116-QP-2014)

Manuscript received 2014-09-09, in revised form 2015-04-07

ABSTRACT

The rather poor oxidation resistance of Nb-Si base ultrahigh temperature alloys has seriously limited their practical applications at high temperatures. Niobium disilicide coatings, especially those modified by reactive elements (RE) such as Zr and Y, have been shown to possess good anti-oxidation properties at high temperatures due to the formation of a protective RE-containing SiO₂ scale.

Halide activated pack cementation (HAPC) is one of the most widely used techniques for preparing protective coatings on Nb-Si base ultrahigh temperature alloys, because compact coatings and metallurgical substrate/coating bonds can be obtained with using this technique. However, only a very limited amount of Zr and Y can be diffused into the coatings by a single co-deposition pack cementation process as a result of their large atomic radii and high melting points. To solve this problem, a method such as magnetron sputtering, which can be used for producing overlay coatings with different composition ratios of coating elements, seems to be feasible. In the present study, ZrSi_2 - NbSi_2 multilayer coatings were prepared on an Nb-Ti-Si-Cr base ultrahigh temperature alloy by first magnetron sputtering 2 μm thick Zr-film, and then Si-Y co-deposition at respectively 1150, 1250 and 1350 $^\circ\text{C}$ by HAPC process. The structures and formation processes, as well as the static oxidation behavior of the coatings were investigated. The results show that the coating prepared at respectively 1150, 1250 and 1350 $^\circ\text{C}$ had similar structures, consisting of a ZrSi_2 outer layer, a $(\text{Nb}, \text{X})\text{Si}_2$ ($\text{X}=\text{Ti}, \text{Cr}, \text{Zr}$ and Hf) middle layer and a $(\text{Ti}, \text{Nb})_5\text{Si}_4$ inner layer. However, the higher co-deposition temperature (1350 $^\circ\text{C}$) could cause cracks at the interfaces between the constituent layers of the coatings. The formation of the coating was dominated by inward diffusion of Si, accompanied with a certain degree of outward diffusion of Nb, Ti and Cr from the base alloy during the second Si-Y co-deposition process. The oxidation tests demonstrated that the ZrSi_2 - NbSi_2 multilayer coating possessed excellent oxidation resistance. After oxidation, a dense scale consisting of SiO_2 , TiO_2 , ZrSiO_4 and Cr_2O_3 formed on the coating, which can protect the base alloy from oxidation at least for 100 h at 1250 $^\circ\text{C}$ in air.

KEY WORDS

Nb-Ti-Si-Cr base ultrahigh temperature alloy, ZrSi_2 - NbSi_2 multilayer coating, structural formation, oxidation-resistant performance

Nb-Si based ultrahigh temperature alloys exhibit great application potential due to their high melting points, low density, and excellent high-temperature strength. However, their poor high-temperature oxidation resistance has seriously limited their practical application as high-temperature structural materials [1,2]. Although multi-element alloying can effectively improve oxidation resistance, this approach has limitations: the addition of large amounts of alloying elements degrades the comprehensive properties of the alloy, such as high-temperature strength and melting point [3,4]. In addition to alloying, surface coating technology is another effective method to improve the oxidation resistance of Nb-Si based alloys. Unlike alloying, surface coating technology improves oxidation resistance with minimal impact on mechanical properties, representing an effective means to promote the practical application of Nb-Si based multicomponent ultrahigh temperature alloys [5~8].

Among protective coatings for Nb-Si based alloys, NbSi_2 coatings have attracted extensive attention due to their low density, high melting point, and good ther-

mal stability. However, pure NbSi₂ coatings cannot meet the requirements for long-term service of Nb-Si based alloys in high-temperature oxidizing environments [6,9]. Previous studies [6,10-12] have shown that the main causes of failure in pure NbSi₂ coatings can be summarized as: (1) NbSi₂ coatings are prone to cracking due to their intrinsic brittleness, providing convenient pathways for inward diffusion of oxygen; (2) the mismatch in thermal expansion coefficients between SiO₂ formed during oxidation and the coating leads to scale spalling during cooling; and (3) consumption of Si in the coating during prolonged oxidation (through outward diffusion to the air/scale interface and inward diffusion to the substrate alloy) results in Si depletion in the residual coating, which cannot sustain the formation of a dense SiO₂ protective scale. In response to these failure mechanisms, researchers worldwide have conducted extensive work aimed at improving the toughness of NbSi₂ coatings, reducing stress in the oxide scale/coating system, and retarding Si consumption, achieving good progress [8,13,14].

Current research focuses on adding modifying elements to the coatings, particularly reactive elements such as Zr and Y, to improve the structure of both the coating and the oxide scale through the reactive element effect [15-17]. Tian and Guo [16] prepared Y-modified silicide coatings and found that Y present in SiO₂ could effectively suppress outward diffusion of Cr, significantly improving high-temperature oxidation resistance compared with simple siliconized coatings. Hong et al. [17] investigated the effect of Zr on the cyclic oxidation resistance of Pt-modified aluminide coatings, demonstrating that Zr addition created a pinning effect at the oxide scale/coating interface, significantly increasing scale adhesion and thereby effectively improving cyclic oxidation resistance.

Pack cementation is an in-situ chemical vapor deposition technique offering flexibility, low production cost, and good repeatability. Moreover, coatings prepared by this method exhibit strong bonding with the substrate alloy, making it suitable for preparing protective coatings on Nb-Si based ultrahigh temperature alloys [14-16,18]. However, due to the large atomic radii and high melting points of Zr and Y, their diffusion into the coating layer is difficult. Consequently, Si-Zr-Y co-diffusion produces coatings with low Zr and Y contents, with these elements mainly distributed in the coating surface region [19]. Magnetron sputtering, on the other hand, can effectively deposit elements with large atomic radii on alloy surfaces [20].

In this work, by combining the characteristics of magnetron sputtering and pack cementation, ZrSi₂-NbSi₂ composite coatings with dense microstructure, high Zr content, strong substrate bonding, and excellent high-temperature oxidation resistance were prepared on Nb-Ti-Si-Cr based ultrahigh temperature alloys through a process of magnetron sputtering a Zr film followed by Si-Y co-diffusion, providing support for the future application of Nb-Si based ultrahigh temperature alloys.

The Nb-Ti-Si-Cr based ultrahigh temperature alloy ingot used in this study was prepared by vacuum arc melting, with a nominal composition (at.%) of Nb-29Ti-8Si-11Cr-4Hf-3Al. Samples measuring 7 mm \times 7 mm \times 7 mm were cut from the master ingot. All surfaces of the samples were ground with SiC abrasive paper up to 1000 grit, ultrasonically cleaned in acetone for 10 min, and then dried with cold air.

The preparation process for the Zr-Y modified silicide composite coating is shown in [Figure 1: see original paper]. First, a Zr film was deposited using a JGP-450 magnetron sputtering system to a thickness of 2 μ m. The specific process parameters were: base vacuum 6.6×10^{-4} Pa, sputtering pressure 1.0 Pa, sputtering power 80 W, and target-to-substrate distance 6 cm.

Si-Y co-diffusion was performed in a self-designed high-temperature, high-vacuum, controlled-atmosphere pack cementation furnace. The preparation process was as follows: samples with deposited Zr films were embedded in a crucible containing the pack mixture, which was then sealed and placed in the furnace. The system was evacuated to 3.0×10^{-2} Pa before heating, and Ar was introduced for protection when the temperature reached 400 $^{\circ}$ C. Based on previous research results from our group [7,14,16,19,21], the pack mixture composition (wt.%) was selected as 10Si-3Y₂O₃-5NaF-82Al₂O₃, with a total mass of 50 g. The mixture was ball-milled for 4 h using a QM-1SP4-CL planetary ball mill. The co-diffusion temperatures were 1150, 1250, and 1350 $^{\circ}$ C, with a holding time of 4 h.

Isothermal oxidation tests of the coated samples were conducted using a self-developed isothermal oxidation furnace at 1250 $^{\circ}$ C in air for 100 h. The phase composition of the coatings and oxide scales was determined using a Panalytical X'Pert PRO X-ray diffractometer (XRD). The microstructure and morphology of the coatings and oxide scales were observed using a Supra-55 scanning electron microscope (SEM), and the local chemical composition was determined using an INCA energy dispersive spectrometer (EDS).

2.1 Microstructure of ZrSi₂-NbSi₂ Composite Coatings

[Figure 2: see original paper] shows cross-sectional SEM-BSE (backscattered electron) images and elemental concentration profiles of the ZrSi₂-NbSi₂ composite coatings prepared by Si-Y co-diffusion at 1150, 1250, and 1350 $^{\circ}$ C for 4 h after magnetron sputtering a 2 μ m thick Zr film. The coatings prepared at different co-diffusion temperatures exhibit similar three-layer structures, each consisting of a gray-white outer layer approximately 5 μ m thick, a relatively thick light-gray intermediate layer, and an inner layer approximately 8 μ m thick. The cross-sectional EDS concentration profiles shown in [Figure 2: see original paper]b, d, and f reveal similar elemental distribution characteristics in each coating: the atomic ratio of Zr to Si in the gray-white outer layer satisfies Zr:Si 1:2. Combined with the XRD spectrum of the coating surface shown in [Figure

3: see original paper] (since all coatings have similar structures and composition distributions, only the XRD spectrum of the coating prepared at 1250 °C is presented) and the Zr-Si binary phase diagram [22], it can be concluded that the outer layer of each coating consists mainly of $ZrSi_2$ phase. In the intermediate layer of each coating, the atomic ratio of (Nb+X) to Si satisfies (Nb+X):Si = 1:2 (X = Ti, Cr, Zr, and Hf), while the composition of the inner layer corresponds to the $(Ti, Nb)_5Si_4$ phase formula. Combined with the XRD spectra of the intermediate and inner layers shown in [Figure 3: see original paper] (the coating was ground from the surface to depths of approximately 20 and 67 μ m for XRD analysis) and the Nb-Ti-Si phase diagram [23,24], the intermediate layer is identified as primarily $(Nb, X)Si_2$, and the inner layer mainly consists of $(Ti, Nb)_5Si_4$ phase.

[Figure 2: see original paper] also shows that while increasing the co-diffusion temperature does not significantly affect the coating structure, it leads to a substantial increase in coating thickness: as the co-diffusion temperature increases from 1150 to 1350 °C, the coating thickness increases from approximately 65 μ m to approximately 120 μ m. Additionally, the coating prepared at 1350 °C exhibits numerous cracks at the interfaces between the constituent layers, with the $ZrSi_2$ outer layer showing obvious fragmentation.

presents the EDS analysis results at the interface between the $ZrSi_2$ outer layer and the $(Nb, X)Si_2$ intermediate layer of the coating prepared at 1250 °C for 4 h. The results show that Nb and relatively high contents of Ti and Cr are present in the $ZrSi_2$ outer layer (point 1 in [Figure 2: see original paper]c), while high contents of Zr, Nb, Ti, and Cr are detected at the interface (point 2 in [Figure 2: see original paper]c). Meanwhile, the Zr content in the $(Nb, X)Si_2$ intermediate layer is approximately 1.1 at.% (point 3 in [Figure 2: see original paper]c). These results indicate that outward diffusion of Nb, Ti, and Cr from the substrate and inward diffusion of Zr occurred during the Si-Y co-diffusion process. This interdiffusion creates elemental gradient distributions at the interfaces between coating layers and between the coating and substrate, which helps reduce internal stresses within the coating and at the coating/substrate interface, resulting in improved interfacial bonding strength and spallation resistance [25].

2.2 Formation Mechanism of $ZrSi_2$ - $NbSi_2$ Composite Coatings

Pack cementation is essentially a chemical vapor deposition technique that forms coatings through solid-state reactive diffusion of the diffusing elements into the substrate alloy [18,26]. Therefore, coating formation is closely related to the diffusion behavior of both the diffusing elements and the constituent elements of the substrate alloy. To further investigate the interdiffusion behavior between the Zr film and substrate alloy at high temperature, samples with a 2 μ m thick magnetron-sputtered Zr film were subjected to interdiffusion treatment at 1250 °C for 4 h. [Figure 4: see original paper] shows the SEM-BSE image and elemental concentration profiles across the Zr film/substrate alloy interface after

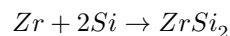
interdiffusion. A distinct interdiffusion zone approximately 3 μm thick formed between the Zr film and substrate alloy, with high contents of Nb, Zr, Ti, and Cr showing obvious gradient distributions along the cross-section. Relatively high contents of Ti, Cr, and Nb were detected in the Zr film, but no Si was present. In contrast, the Zr content in the substrate alloy was only about 1.2 at.%, mainly confined to the surface region of the substrate. These results demonstrate that coating formation is dominated by inward diffusion of Si, accompanied by a certain degree of outward diffusion of Nb, Ti, and Cr from the substrate alloy, while the diffusion rate of Zr in the substrate alloy is relatively slow.

The melting point T is an important parameter for diffusion activation energy Q [27]. The melting point of Zr (2125 K) is much higher than that of Si (1685 K). According to the empirical relationship $Q = 32T$, the activation energy required for Zr diffusion is much greater than that for Si, meaning the diffusion coefficient of Zr is far smaller than that of Si [28,29]. The diffusion process follows Fick's first and second laws, and the average diffusion distance L of atoms during diffusion is given by [27]:

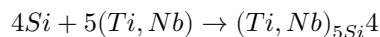
$$L = C\sqrt{Dt}$$

where t is diffusion time, C is a constant determined by geometric factors, and D is the diffusion coefficient. Therefore, coating growth is dominated by inward diffusion of Si, while Zr diffusion is more difficult and occurs over shorter distances.

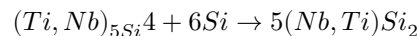
During the initial stage of coating growth, Si atoms adsorbed on the sample surface first react with the outermost Zr film as follows:



After the Zr film is completely converted to ZrSi_2 , the continuously inward-diffusing Si reacts with the Nb-Ti-Si-Cr substrate. It should be noted that since the formation enthalpy of Ti_5Si_4 phase (-597 kJ/mol) [30] is lower than those of NbSi_2 and TiSi_2 phases (-161 [31] and -160 [32] kJ/mol, respectively), the active Si atoms first react with Nb and Ti elements in the substrate:



forming $(\text{Ti}, \text{Nb})_{5\text{Si}_4}$ (the solubility of Nb in Ti_5Si_4 phase exceeds 47% at 1250 $^\circ\text{C}$ [24]), which then reacts with continuously diffusing Si atoms:



With sustained inward diffusion of Si, the $(\text{Ti}, \text{Nb})_{5\text{Si}_4}$ phase advances as a diffusion front into the substrate alloy. The relationship between the diffusion

coefficient of Si and temperature can be described by the Arrhenius equation [27]:

$$D = D_0 \exp\left(-\frac{Q}{RT}\right)$$

where D_0 is the diffusion constant, R is the molar gas constant, and T is the thermodynamic temperature. Thus, increasing temperature leads to an exponential increase in Si diffusion rate, resulting in a significant increase in coating thickness.

It should be pointed out that reactions (2)–(4) all cause volume expansion, with different degrees of expansion for different reactions. For example, reaction (2) causes approximately 2.15% volume expansion, while reaction (4) causes about 2.35% expansion. These differences in volume expansion introduce significant internal stresses at the interfaces between the coating and substrate and between the constituent coating layers. Additionally, differences in thermal expansion coefficients between the coating layers and between the coating and substrate also introduce internal stresses during cooling. The increased coating thickness and accelerated growth rate caused by higher co-diffusion temperatures exacerbate these internal stresses, leading to crack formation within the coating, particularly at the interfaces between layers. Therefore, coatings prepared at 1150 and 1250 °C...

2.3 High-Temperature Oxidation Behavior of ZrSi₂-NbSi₂ Composite Coatings

[Figure 5: see original paper] shows the macroscopic morphology, surface SEM-BSE image, and XRD spectrum of the ZrSi₂-NbSi₂ composite coating prepared by Si-Y co-diffusion at 1250 °C for 4 h after magnetron sputtering a Zr film, following isothermal oxidation at 1250 °C in air for 100 h. The results show that after oxidation at 1250 °C for 100 h, the coating surface remained intact with a dense oxide scale. The surface XRD spectrum ([Figure 5: see original paper]b) reveals that the oxide scale consists mainly of a mixture of SiO₂, TiO₂, and ZrSiO₄ phases. This demonstrates that the prepared ZrSi₂-NbSi₂ composite coating possesses excellent high-temperature oxidation resistance, capable of protecting the substrate alloy from oxidation in air at 1250 °C for at least 100 h.

[Figure 6: see original paper] presents cross-sectional SEM-BSE images of the coating after oxidation at 1250 °C for 100 h. The ZrSi₂ outer layer has completely disappeared, and a dense oxide scale approximately 30 μm thick has formed on the surface. This oxide scale consists of a mixture of black glassy phase, white particulate phase dispersed in the outer region of the scale, flaky gray phase, and continuous light-gray phase at the bottom of the scale. The EDS analysis results for these typical microstructures are shown in . The black glassy phase contains up to 22.6 at.% Si, indicating it is SiO₂ (although SiO₂

exists mainly in amorphous form and thus shows weak XRD peaks despite its high content in the scale). The white particulate phase in the outer region of the scale contains approximately 14.1 at.% Zr and 14.4 at.% Si, while the composition of the flaky gray phase corresponds to the TiO_2 formula. Combined with the surface XRD spectrum of the scale ([Figure 5: see original paper]b), the white particulate phase is identified as mainly ZrSiO_4 , and the flaky gray phase as mainly TiO_2 . [Figure 7: see original paper] shows the calculated Gibbs free energy curves for the reaction $\text{ZrO}_2 + \text{SiO}_2 \rightarrow \text{ZrSiO}_4$ at different temperatures. The results indicate that ZrSiO_4 formation satisfies the thermodynamic conditions during oxidation. Kaiser et al. [33] and Ebener et al. [34] also reported that ZrSiO_4 can form slowly at temperatures above 1200 °C. Since ZrSiO_4 is chemically stable and its formation causes approximately 7% volume contraction, it can help reduce internal stresses caused by thermal expansion coefficient mismatch between the oxide scale and the remaining coating, thereby improving scale spallation resistance. The continuous gray phase at the bottom of the scale contains about 29.5 at.% Cr, indicating it is mainly Cr_2O_3 . This suggests that outward diffusion of elements was suppressed during oxidation. Previous studies [35] have shown that reactive elements such as Zr and Y tend to segregate at oxide grain boundaries, hindering outward diffusion of metallic elements like Nb, Ti, and Cr to the air/scale interface and transforming the dominant diffusion mechanism from outward metal diffusion to inward O^{2-} diffusion. Since the diffusion rate of O^{2-} in a dense oxide scale is significantly lower than that of metallic elements, this transformation in diffusion mechanism can substantially reduce the oxide scale growth rate and enhance the high-temperature oxidation resistance of the coating [36].

[Figure 6: see original paper]b also reveals that numerous pores formed in the coating beneath the oxide scale, and the coating thickness increased significantly from approximately 65 μm before oxidation to about 125 μm . The thickness of the $(\text{Ti, Nb})_5\text{Si}_4$ inner layer increased markedly, while that of the $(\text{Nb, X})\text{Si}_2$ intermediate layer decreased. These changes in the coating were mainly caused by outward diffusion of Si, Ti, and Cr during oxidation, as well as continued inward diffusion of Si into the substrate alloy. Previous studies [10] have shown that when the Si content in the coating exceeds 40 at.%, a continuous SiO_2 scale can form. Therefore, the persistence of the $(\text{Nb, X})\text{Si}_2$ layer in the remaining coating indicates that the prepared $\text{ZrSi}_2\text{-NbSi}_2$ composite coating still has further oxidation resistance potential.

Conclusions

- (1) $\text{ZrSi}_2\text{-NbSi}_2$ composite coatings were successfully prepared on Nb-Ti-Si-Cr based ultrahigh temperature alloys by a process involving magnetron sputtering of a Zr film followed by Si-Y co-diffusion. Coatings prepared at different Si-Y co-diffusion temperatures exhibited similar structures, consisting mainly of a ZrSi_2 outer layer, a $(\text{Nb, X})\text{Si}_2$ intermediate layer, and a $(\text{Ti, Nb})_5\text{Si}_4$ inner layer. The coating thickness increased significantly

with increasing co-diffusion temperature, but excessively high co-diffusion temperatures caused crack formation between the constituent layers.

- (2) Coating formation was dominated by inward diffusion of Si, accompanied by a certain degree of outward diffusion of Nb, Ti, and Cr from the substrate alloy.
- (3) The prepared $\text{ZrSi}_2\text{-NbSi}_2$ composite coatings exhibited excellent high-temperature oxidation resistance. After oxidation, a dense oxide scale composed of SiO_2 , TiO_2 , ZrSiO_4 , and Cr_2O_3 formed on the coating surface, which protected the substrate alloy from oxidation in air at $1250\text{ }^\circ\text{C}$ for at least 100 h.

References

- [1] Bewlay B P, Jackson M R, Zhao J C, Subramaniam P R. *Metall Mater Trans*, 2003; 34A: 2043
- [2] Guo X P, Gao L M, Guan P, Kusabiraki K, Fu H Z. *Mater Sci Forum*, 2007; 539-543: 3690
- [3] Murayama Y, Hanada S. *Sci Technol Adv Mater*, 2002; 3: 145
- [4] Zelenitsas K, Tsakiroopoulos P. *Mater Sci Eng*, 2006; A416: 269
- [5] Vilasi M, Steinmetz J, Allemand B G. *J Adv Mater*, 2000; 32: 53
- [6] Suzuki R O, Ishikawa M, Ono K. *J Alloys Compd*, 2002; 336: 280
- [7] Tian X D, Guo X P. *Acta Metall Sin*, 2008; 44: 585 (田晓东, 郭喜平. *金属学报*, 2008; 44: 585)
- [8] Zhang P, Guo X P. *Corros Sci*, 2013; 71: 10
- [9] Majumdar S, Sengupta T P, Kale G B, Sharma I G. *Surf Coat Technol*, 2006; 200: 3713
- [10] Cockeram B V, Rapp R A. *Mater Sci Eng*, 1995; A192: 980
- [11] Dzyadikovich Y V, Kitskai L I. *Powder Metall Met Ceram*, 1997; 36: 77
- [12] Yoon J K, Kim G H, Han J H, Shon I J, Doh J M, Hong K T. *Intermetallics*, 2005; 13: 1146
- [13] Christensen R J, Tolpygo V K, Clarke D R. *Acta Mater*, 1997; 45: 1763
- [14] Qiao Y Q, Guo X P. *Appl Surf Sci*, 2010; 256: 7462
- [15] Wang W, Yuan B F, Zhou C G. *Corros Sci*, 2014; 80: 164
- [16] Tian X D, Guo X P. *Surf Coat Technol*, 2009; 204: 313
- [17] Hong S J, Hwang G H, Han W K, Lee K S, Kang S G. *Intermetallics*, 2010; 18: 864
- [18] Xiang Z D, Datta P K. *Acta Mater*, 2006; 54: 4453
- [19] Li X, Guo X P. *Acta Metall Sin*, 2012; 48: 1394 (李轩, 郭喜平. *金属学报*, 2012; 48: 1394)
- [20] Kelly P J, Brien J O, Arnell R D. *Vacuum*, 2004; 74: 1
- [21] Zhang P, Guo X P. *Acta Metall Sin*, 2010; 46: 821 (张平, 郭喜平. *金属学报*, 2010; 46: 821)
- [22] Salpadoru N H, Flower H M. *Metall Mater Trans*, 1995; 26A: 243
- [23] Wang R C, Jin Z P, Liu C L. *J Cent South Univ Technol*, 2002; 33: 385 (王日初, 金展鹏, 柳春雷. *中南工业大学学报*, 2002; 33: 385)
- [24] Zhao J C, Jackson M R, Peluso L A. *Mater Sci Eng*, 2004; A372: 21

- [25] Sanjib M, Indrakumar S, Indradev S, Parag B. J Electrochem Soc, 2008; 155D: 743
- [26] Cockeram B V, Rapp R A. Metall Mater Trans, 1995; 26A: 777
- [27] Pan J S, Tong J M, Tian M B. Fundamentals of Materials Science. Beijing: Tsinghua University Press, 1998: 466 (潘金生, 仝建民, 田民波. 材料科学基础. 北京: 清华大学出版社, 1998: 466)
- [28] Patil R V, Kale G B, Garg S P. J Nucl Mater, 1995; 223: 169
- [29] Milanese C, Buscaglia V, Maglia F, Tamburini U A. Acta Mater, 2003; 51: 4837
- [30] Colinet C, Tedenac J C. Intermetallics, 2010; 18: 1444
- [31] Fernandes P B, Coelho G C, Ferreira F, Nunes C A, Sundman B. Intermetallics, 2002; 10: 993
- [32] Pelleg J, Shor Y. Microelectron Eng, 2003; 69: 65
- [33] Kaiser A, Lobert M, Telle R. J Eur Ceram Soc, 2008; 28: 2199
- [34] Ebener S, Winter W. J Eur Ceram Soc, 1996; 16: 1179
- [35] Moon D P. Mater Sci Technol, 1989; 5: 754
- [36] Thanneeru R, Patil S, Deshpande S, Seal S. Acta Mater, 2007; 55: 4117

Note: Figure translations are in progress. See original paper for figures.

Source: ChinaXiv — Machine translation. Verify with original.